*J. Physiol.* (1980), **309**, *pp.* 287–315
*With* 14 *text-figures*
*Printed in Great Britain*



# BEHAVIOUR OF THE ROD NETWORK IN THE TIGER SALAMANDER RETINA MEDIATED BY MEMBRANE PROPERTIES OF INDIVIDUAL RODS

BY DAVID ATTWELL AND MARTIN WILSON

*From 253 Cory Hall, Graduate Group in Neurobiology, Department of Electrical Engineering and Electronics Research Laboratory, University of California, Berkeley, California 94720, U.S.A.*

(*Received 17 December 1979*)

SUMMARY

1. The spread of electrical signals between rods in the salamander retina was examined by passing current into one rod and recording the voltage responses in nearby rods. Rod network behaviour, measured in this way, was simulated from data on rod membrane properties gathered in voltage-clamp experiments on single isolated rods.

2. The network voltage responses to square current pulses became smaller, more transient, and had a longer time-to-peak, for rods further away from the site of current injection. Depolarizing currents produced smaller responses than hyperpolarizing currents of the same magnitude.

3. Neighbouring rods and cones were coupled less strongly than neighbouring rods.

4. The response of the rod network to current injection was unaffected by 2 mM-aspartate$^-$, which eliminates transmission from receptors to horizontal cells.

5. The input resistance of single isolated rods, measured at the resting potential, varied between 100 and 680 MΩ. The lower values were probably due to damage by the micro-electrodes. Electrical coupling was found to be very strong between the rod inner and outer segments.

6. A strong 'instantaneous' outward rectification seen in isolated rods at potentials positive to $-35$ mV was reduced, but not abolished, by 15 mM-TEA.

7. In normal solution, isolated rods exhibited a voltage- and time-dependent current, $I_A$, whose kinetics were approximated by a single first-order gating variable, and whose activation curve spanned the range between $-40$ and $-80$ mV. The time constant for the current varied with voltage and was 60–200 msec between $-140$ and $-40$ mV.

8. A reversal potential for $I_A$ could not be found between $-140$ and $-40$ mV in normal solution, and the fully activated current, $\bar{I}_A$, was approximately voltage-independent, with a magnitude of $\sim$ 0·1 nA over this potential range.

9. By several criteria, $I_A$ behaved as a single inward current activated by hyperpolarization. Pharmacological studies suggest, however, that it is the sum of at least two currents with very similar kinetics.

10. Most isolated rods exhibited a very slow ($\tau \sim 3$ sec) increase in net outward

0022-3751/80/2920-0667 $07.50 

current on depolarizing beyond $-35$ mV. The magnitude of this current varied considerably between cells.

11. Assuming that the rod network can be approximated by a square lattice of individual rods, resistively coupled together, the voltage-clamp data on isolated rods were used to predict the response of the network to current injection at one cell. The theoretical and observed network behaviour were in good agreement. The resistance coupling neighbouring rods was estimated to be $\sim 300$ MΩ. The current $I_A$ plays a major role in determining the behaviour of the rod network.

12. The time-dependent current, $I_A$, is responsible for the peak–plateau wave form of the response to a bright flash. A current similar to $I_A$ could also account for the negative propagation velocity of the peak of the dim flash response, through the rod network of the turtle, observed by Detwiler, Hodgkin & McNaughton (1978).

## INTRODUCTION

In the vertebrate retina, single photoreceptors do not behave as independent light transducers, but instead are coupled, probably electrically, to other photoreceptors nearby (Baylor, Fuortes & O'Bryan, 1971; Fain, 1975; Schwartz, 1975*a*, *b*, 1976; Copenhagen & Owen, 1976; Werblin, 1978; Gold & Dowling, 1979; Gold, 1979). Quanta absorbed by one receptor can produce an electrical response in a receptor some distance away.

The mosaic of coupled receptors has been treated theoretically by assuming that there are resistive connexions between neighbouring cells, and that each cell's membrane has a linear current–voltage relationship (Lamb & Simon, 1976; Schwartz, 1976; Gold, 1979). There are, however, strong indications that this approach is not always valid.

Schwartz (1975*a*, 1976) found that in the turtle rod network, the voltage response to a large spot of light can become transiently less than the voltage response to a small spot of light during the decaying phase of the response. This effect was shown to involve electrical coupling between rods, but is not compatible with a resistive and capacitative model of the network.

Striking evidence for the inadequacy of the resistive and capacitative model has come from measurements of the speed of propagation of signals through the rod network of the turtle retina (Detwiler, Hodgkin & McNaughton, 1978). These authors found that the time to reach peak voltage, following the onset of a flash, was shorter in rods further away from a bar of light. This surprising result was modelled by the introduction of inductive elements into a resistive network. While, formally, this model is adequate to fit their data, it does not illuminate the mechanism of the effect, nor is it generally applicable. As Detwiler *et al.* (1978) suggested, the 'inductor' in their model probably corresponds to voltage-dependent conductances in the rods themselves. Recent studies have shown that the rods do indeed possess strong voltage-dependent properties (Fain, Quandt & Gerschenfeld, 1977; Bader, MacLeish & Schwartz, 1978; Fain, Quandt, Bastian & Gerschenfeld, 1978; Werblin, 1979). In this paper we examine the proposition that the unusual properties of the rod network are determined by the voltage-dependent properties of individual rods.

The membrane properties of individual rods have been analysed using the voltage-clamp technique on isolated cells, and signal spread in the rod network has been measured by injecting current into one rod and recording voltage in another rod. A third section of this work combines both sets of experimental results in a simulation of the rod network behaviour using the data obtained from voltage-clamp experiments on single rods.

## METHODS

### *Preparation*

Experiments were carried out on larval tiger salamanders, *Ambystoma tigrinum*, using either the flat-mounted isolated retina or the retinal slice preparations described in detail by Werblin (1978). Dissections were performed in dim red light, and the preparations, when mounted under the microscope for electrode insertion, were illuminated with red light (Kodak Wratten filter 92). Light responses in rods, either isolated or in the network, were not routinely checked.

Recording and voltage-clamp techniques were modified from those of Werblin (1975) to allow the use of two separate micro-electrodes. Clamp current was measured from the voltage drop across a $10^{10}$ Ω resistor in series with the current-passing electrode. The electrodes used typically had resistances of 130 MΩ when filled with 4 M-potassium acetate. Each electrode was independently inserted into a receptor, under visual control, by setting into oscillation the negative capacity compensation of the preamplifier. Hoffman Modulation contrast optics (Modulation Optics Inc., Greenvale, N.Y.) were used to facilitate seeing the cells and electrodes. The use of visual control of the electrodes' positions allowed us to be completely certain about which cells were being impaled (except for experiments on rod–cone coupling in the network: see p. 293). Separate bath electrodes were used for voltage recording and current passing.

Single rods used in the voltage-clamp experiments were obtained by the method of Werblin (1978). An isolated retina was cut into thin slices with a razor blade, during which procedure a few rods usually become detached from the rest of the retina. These entirely isolated rods were without axons, but apparently were not otherwise damaged. The membrane at the point where the axon detached apparently sealed over well, because the rod input resistance was similar to that found by Bader *et al.* (1978) for intact isolated cells. Recordings were made only from those isolated cells having smooth inner and outer segments and clear cytoplasm. Poor electrode penetrations were often accompanied by the rapid formation of circular marks in the rod, centred around the electrode tip and possibly representing newly-formed vacuoles. The apparent input resistance in cells showing such marks was abnormally low ($< 100$ MΩ), but could be improved if the electrodes were removed and re-inserted.

In this study the coupling between eighty-seven pairs of rods in the isolated retina was measured, and ninety-three isolated rods were voltage-clamped, of which forty-one were analysed as described in section *B*. Although both 'red' and 'green' rods occur in the salamander retina (Walls, 1942, p. 599), we estimate 'green' rods to be less than a tenth as numerous as 'red' rods (based on rod colour seen in freshly isolated retinae). 'Green' rod tips lie below those of 'red' rods, and are unlikely, therefore, to have been impaled in the isolated retina. 'Green' rods, defined by the morphology described by Walls (1942, p. 599), were not voltage-clamped.

### *Solutions*

Preparations were maintained at room temperature (24–27 °C) in an oxygenated medium, similar to that used by Dennis & Sargent (1979), comprising Leibovitz L-15 synthetic culture medium (GIBCO, Grand Island, N.Y.) made up to 38% normal strength, to which supplementary ions were added. The calculated final concentrations (mM) of the major constituents were: NaCl, 104; KCl, 2·1; $CaCl_2$, 3·6; $Na_2HPO_4$, 0·5; $MgCl_2$, 0·4; $MgSO_4$, 0·3; glucose, 5; HEPES, 5; pH adjusted to 7·6. The osmolarity of this solution (223 m-osmole/kg, measured with a vapour pressure osmometer) is 5% higher than that of the solution used conventionally for the salamander retina (Marshall & Werblin, 1978). This medium was found to give much healthier, longer-lasting preparations, and significantly increased the success rate of the experiments. 15 mM-tetra-ethylammonium chloride (TEA) replaced the same molarity of NaCl in some

experiments, but when other drugs or ions have been used, they were simply added to the normal medium. It was not practical to change the composition of the perfusing medium while the electrodes were in cells. Data given in different media were obtained from different cells.

*Clamp quality*

(1) *Settling time.* When voltage-clamping isolated rods, after a step change of the command potential by an amount $\Delta V$, the membrane potential altered by at least 95% of $\Delta V$ within 10 msec.

(2) *Voltage uniformity.* We have considered two possible causes of voltage non-uniformity.

(*a*) Even ignoring the presence of a resistive junction between the inner and outer segments, there will be longitudinal non-uniformity of potential due to axial resistance along the rod cytoplasm. Calculations indicate that this is negligible along the rod inner segment, but it can be significant along the outer segment, where axial current must largely flow along the thin annulus between the surface membrane and the outer surface of the disks. Assuming the thickness of this annulus to be 26 nm (Brown, Gibbons & Wald, 1963, fig. 2*b*; Sjöstrand & Kreman, 1978, p. 224), the cytoplasm resistivity to be 2 Ωm and the rod outer segment resistance at the resting potential to be 900 MΩ (i.e. about twice the total rod resistance), then for an outer segment of length $L = 30$ μm and radius 6 μm one can estimate a space constant of $\lambda \simeq 115$ μm. From linear cable theory, if current is injected into one end of a cable of length $L$, and space constant $\lambda$, and the other end of the cable is sealed, the fractional variation of voltage along the cell is $\Delta V/V = (1+e^{2L/\lambda}-2e^{L/\lambda})/(1+e^{2L/\lambda})$. Using the values above for $L$ and $\lambda$ we find $\Delta V/V \sim 0{\cdot}033$, and the voltage is essentially uniform. For potentials positive to $-35$ mV, however, where the outer segment membrane resistance may be as low as 20 MΩ (assuming the outward rectifying channels to be uniformly distributed over the rod), $\lambda$ may be $\sim 17$ μm so that $\Delta V/V \simeq 0{\cdot}66$ and the voltage is extremely non-uniform. Such non-uniformity will distort the kinetics and amplitudes of the time-dependent currents observed.

(*b*) The resistance of the stalk between the inner and outer segments will also tend to produce voltage non-uniformity. We have verified directly (see Results) that this resistance is small compared to the rod resistance at the resting potential, but our data only allow us to say that the resistance is less than $\sim$ 15 MΩ. It is possible, therefore, that this resistance contributes to the severe voltage non-uniformity which may occur for pulses positive to $\sim -35$ mV, when the rod resistance falls to $\sim$ 10 MΩ.

*Computing*

The simultaneous differential equations describing the rod network were solved in two ways: (1) by the Adams–Moulton difference method, using the programme 'EPISODE' (Hindmarsh & Byrne, 1977), which automatically adjusts the time interval used in the integration to achieve any desired accuracy; (2) by the Euler method, with very small time increments (0·1 msec for negative pulses, 0·01 msec for positive pulses). Decreasing the 'error parameter' for the EPISODE programme or the time increment used for the Euler method by a factor of 10 affected the solutions by less than 1% at all times. The solutions obtained with the two methods agreed to within the thickness of the lines in the figures shown.

## RESULTS

### *A. Properties of the rod network*

*Choice of network model and nomenclature*

The distribution of receptors in the salamander retina does not correspond exactly to any regular lattice geometry. Fig. 1*A* is taken from a tracing of a photomicrograph of an isolated retina, viewed from the receptor side and focused at the level of the outer segments. There are approximately equal numbers of rods and cones, distributed fairly evenly across the figure.

From direct observation of gap junctions between rods, Gold (1979) estimated

that on average every red rod is connected to 4·6 others in the toad retina. Since salamander rods are probably similarly coupled through gap junctions (Custer, 1973), a similar pattern of coupling may well exist in our preparation. Consequently we have followed Gold (1979) and used a square lattice, with connexions between nearest neighbours, as an idealized description of the rod network. The nomenclature for this lattice is shown in Fig. 1*B*. The rod into which current is injected is defined as $\text{rod}_{0,0}$.

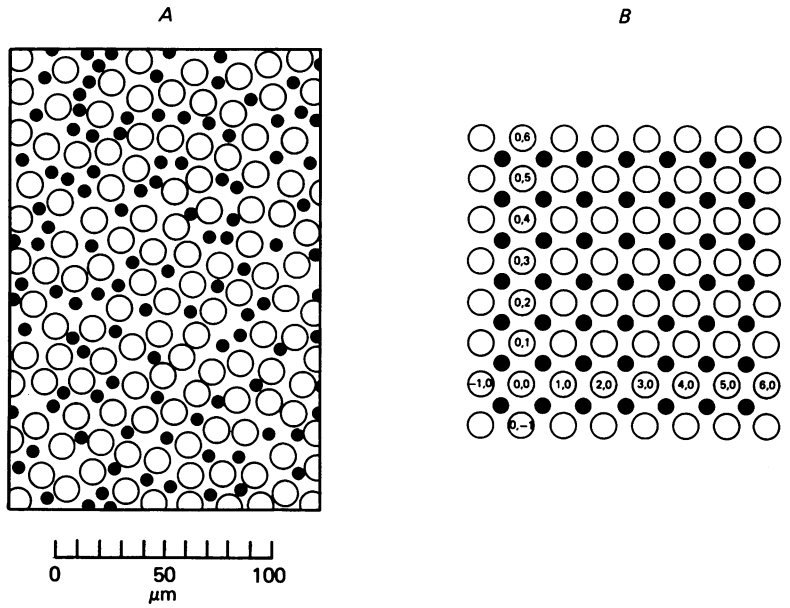


Fig. 1. Comparison of actual and idealized arrangement of receptors in the retina. *A*, actual arrangement, taken from a photomicrograph of an isolated flat-mounted retina focused at the level of the outer segments. The 120 rod outer segments in the field are shown as large open circles. The 107 cone outer segments are shown as small filled circles. Double cones are shown as single circles. *B*, idealized arrangement of receptors assumed for computing the network behaviour. Cones (filled circles) occupy the interstices of the square rod lattice (open circles). $\text{Rod}_{0,0}$ is the rod into which current is injected. Next neighbour rods are assumed to be coupled, so that $\text{rod}_{0,0}$ is coupled to $\text{rod}_{1,0}$, $\text{rod}_{0,1}$, $\text{rod}_{-1,0}$ and $\text{rod}_{0,1}$. Diagonal neighbours (e.g. $\text{rod}_{0,1}$ and $\text{rod}_{1,0}$) are assumed not to be directly coupled.

The positions of other rods are defined by their lattice positions with respect to $\text{rod}_{0,0}$. In the experiments on the network, these positions were obtained by direct visual inspection, though there is sometimes ambiguity in this labelling because of irregularities in the lattice geometry (Fig. 1*A*). The potential in $\text{rod}_{i,j}$ is defined to be $V_{i,j}$.

*The response of the network to current injection*

The properties of the rod network were investigated using the isolated flat-mounted retina preparation (Werblin, 1978). The basic experiment performed was the injection of square current pulses into one rod, while recording the voltage in another rod or in the same rod.

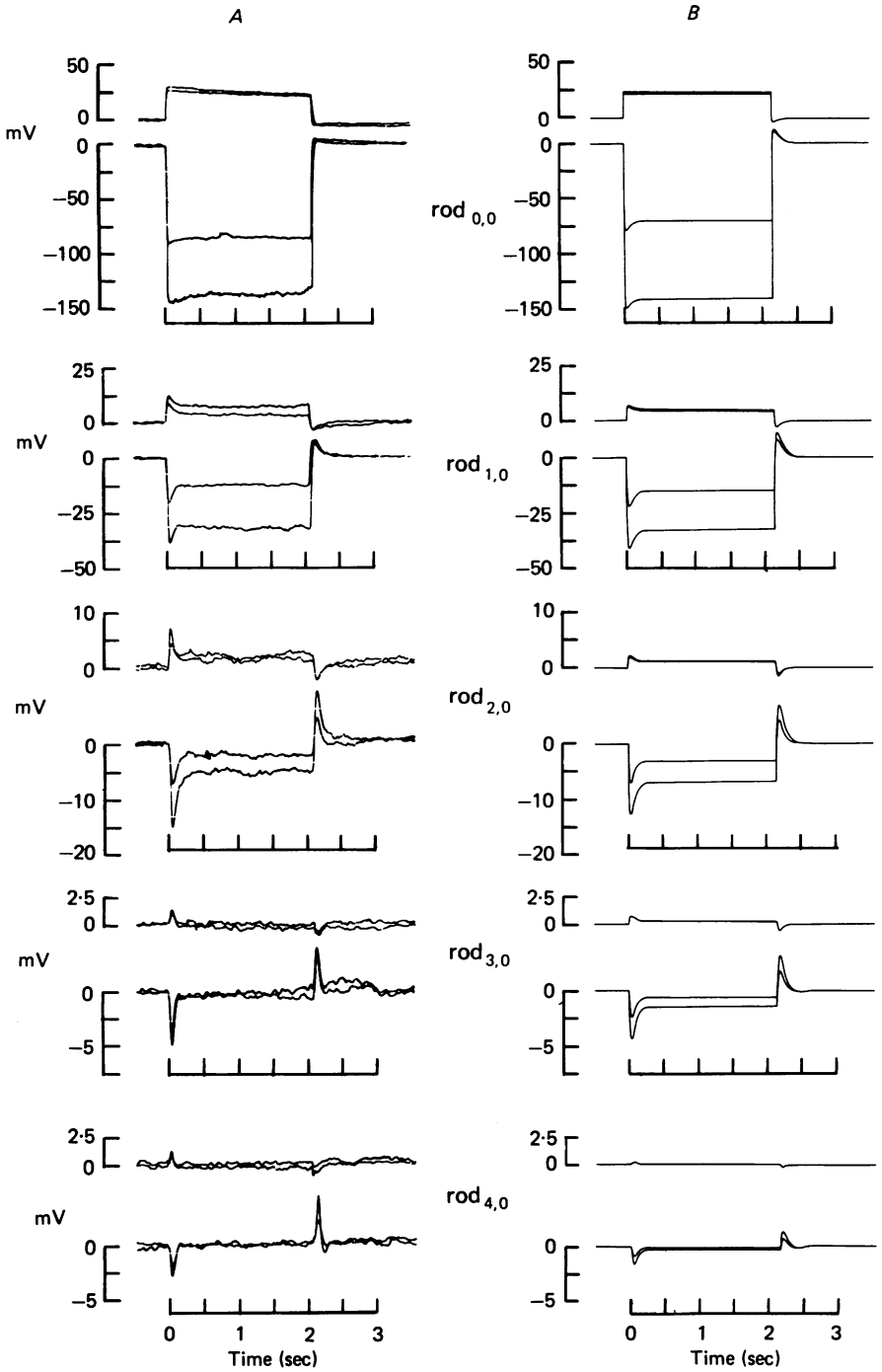


Fig. 2. Measured and computed voltage responses of the rod network to injection of ± 1 and ± 2 nA current pulses into $rod_{0,0}$. Potentials measured with respect to resting potential. Pulse length was 2·14 sec. *A*, responses of rods at different distances from $rod_{0,0}$ (see Fig. 1*B* for nomenclature). At greater distances the responses become smaller and more transient, with a longer time-to-peak (e.g. for the 1 nA hyper-

The voltage response of $rod_{0,0}$, shown in Fig. 2*A*, was qualitatively similar to that described by Werblin (1978). The major features of the response were a strong outward rectification at potentials positive to $\sim -35$ mV and a slow sag in potential for negative-going pulses. In addition there was a time-independent inward rectification negative to about $-120$ mV. Typically, the input resistance measured at $rod_{0,0}$ was 90 MΩ, somewhat lower than reported by Lasansky & Marchiafava (1974) but about the same as found by Schwartz (1976), and higher than found by Werblin (1978).

Voltage responses in excess of 1 mV could regularly be recorded as far as four cells distant from $rod_{0,0}$ when the maximum hyperpolarizing current of 2 nA was injected. Fig. 2*A* shows typical results obtained from $rod_{1,0}$ to $rod_{4,0}$. The voltage signal became progressively smaller, further away from the injected rod, and there were systematic changes in the shape of the response with distance. These changes can be summarized as an enhancement of the peak ('make' and 'break') potentials relative to steady-state potentials, and a slowing of the times-to-peak.

To investigate the possibility that signal shaping in the rod network involves horizontal cells, experiments were performed in the presence of 2 mM-sodium aspartate, which eliminates horizontal cell activity (Cervetto & MacNichol, 1972; Brown & Pinto, 1974; Normann & Pochobradský, 1976). Recordings were made from at least two cells at each rod position from $rod_{0,0}$ to $rod_{4,0}$. No significant difference could be detected in this medium. In agreement with Owen & Copenhagen (1977) and Schwartz (1976), we conclude that signal spread and shaping in the rod network does not involve the activity of horizontal cells.

*Coupling of rods and cones*

As well as gap junctions between the interdigitating fins of salamander rods, gap junctions between rods and cones have been described (Custer, 1973). Although these junctions are probably smaller and less numerous than rod–rod junctions (Gold & Dowling, 1979), they nevertheless suggest coupling between rods and cones. In order to examine this possibility directly, the experimental protocol used to investigate rod–rod coupling was also applied to rods and cones.

Some experiments were carried out on the isolated flat retina, but this method was unsatisfactory because the cone tips are small and lie below the tips of the rod outer segments, and it was not always possible to be confident that the electrode had penetrated a cone rather than a neighbouring rod. Thus, the majority of these experiments were done using the retinal slice preparation (Werblin, 1978). The coupling measured between a rod and a directly adjacent cone was between one quarter and one half as strong as that between directly adjacent rods in the slice preparation (Fig. 3). Directly adjacent rods were apparently coupled more strongly in retinal slices than in the isolated flat-mounted retina, presumably because rod–rod connexions severed by the slicing procedure sealed over with a high resistance

polarizing pulse the time to peak was 44 msec at $rod_{0,0}$ and 70 msec at $rod_{4,0}$). Depolarizing currents gave smaller responses than hyperpolarizing currents of the same magnitude. On terminating the 2 nA hyperpolarizing current pulse, the potential in $rod_{4,0}$ initially showed a positive overshoot which was followed by a small, but consistently observed, negative undershoot. *B*, predicted network responses based on voltage-clamp data from isolated rods (see section *C* in text for details).

membrane, decreasing the number of paths available for current flow away from the site of current injection.

Rod–cone coupling has also been observed, using less direct techniques, in the turtle (Schwartz, 1975*b*) and in the toad (Fain, 1976).

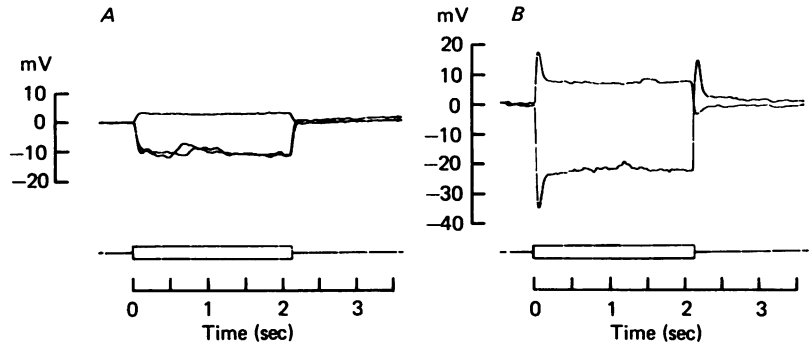


Fig. 3. Voltage responses of a single cone (*A*) and a rod (*B*) to the injection of ± 1 nA (lower trace) into an immediately adjacent rod in the retinal slice preparation. Rod–rod coupling in the slice was apparently stronger than in the intact isolated retina (cf. Fig. 2*A*). Rod–cone coupling was weaker than rod–rod coupling.

### *B. The membrane properties of isolated rods*

Experiments were carried out on rods isolated from the retinal slice preparation. Both electrodes were usually inserted in the inner segment, since this is easier to penetrate, but some experiments were done with one electrode in the inner and one in the outer segment. No significant difference was found. The holding potential ($V_H$) was usually the resting potential (−45 to −70 mV), but experiments were sometimes also done using a more negative $V_H$.

#### *Voltage uniformity*

The adequacy of the voltage-clamp technique to investigate membrane currents depends critically on the whole membrane experiencing the same potential. It has been suggested (Werblin, 1975; Cervetto, Pasino & Torre, 1977) that the narrow connexion between the inner and outer segments of the rod constitutes a high resistance, which isolates the two segments. More recent evidence argues against this proposition (Werblin, 1978; Bader *et al.* 1978), but since this point is crucial it has been examined directly in experiments like the one shown in Fig. 4. Two microelectrodes were placed in the outer segment of an isolated rod and the voltage response to a small current pulse was measured. The voltage electrode was then carefully withdrawn and re-inserted in the inner segment, where the voltage response to the same current pulse into the outer segment was measured. In this and two similar experiments the response to the current pulse was not significantly different in the two cases, confirming that the inner and outer segments are very well coupled. For the experiment in Fig. 4 we estimate that the response in the two segments differs by less than 5 %. Assuming that the membrane resistances of the two segments

are equal, we therefore calculate the coupling resistance between the two segments to be less than 15 MΩ. A cytoplasmic stalk of resistivity 2 Ωm having the dimensions of the bridge between the two segments (Brown *et al.* 1973, Fig. 2*A*), would have a resistance of about 12 MΩ.

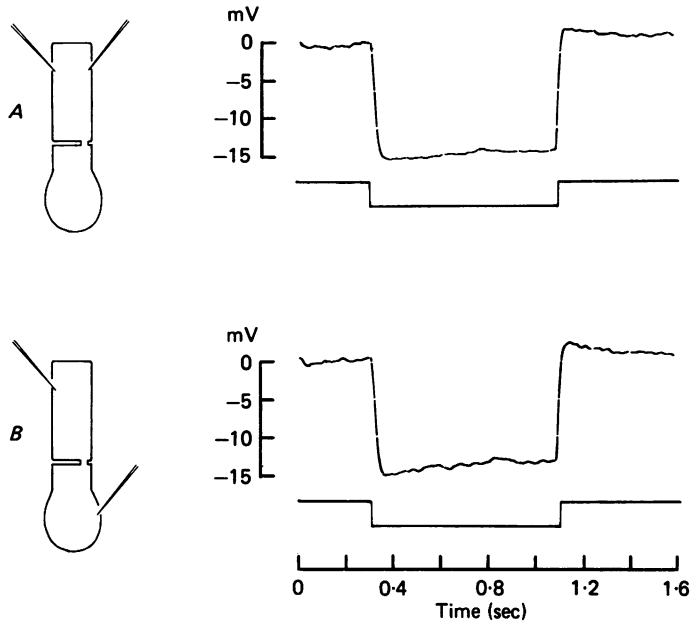


Fig. 4. Voltage responses in the outer (*A*) and inner (*B*) segments of an isolated rod, when −0·1 nA was injected into the outer segment. The voltage responses were not significantly different, showing that the outer and inner segments were well coupled. Resting potential −45 mV.

*Membrane capacitance*

The membrane capacitance was calculated from the slope resistance and the time constant of the voltage response to a square current pulse. To avoid errors arising from gating changes during the voltage response, the square current pulse was superimposed on a constant current which hyperpolarized the membrane to −100 mV (a potential range where no gating changes are thought to occur: see Fig. 8*D*). The membrane *I–V* relation was essentially linear over the voltage range used for this measurement (−110 to −90 mV), and the membrane time constant was the same for depolarizing and hyperpolarizing pulses. In two cells the capacitance was found to be 39·8 and 40·2 pF. For a typical rod of length 57 $\mu$m (without axon) and diameter 12·5 $\mu$m (averaged over the length of the rod), this gives a specific capacitance of 1·6 $\mu$F/cm$^2$ of cell membrane.

In this calculation we treat the rod as a cylinder of the dimensions given. Including the membrane area comprising (1) the outer end of the inner segment, (2) the inner end of the outer segment, and (3) the few disks with access to the extracellular space, would lower this value slightly.

*'Instantaneous' and steady-state I–V relations*

The $I-V$ relations determined 10 msec (●) and 3 sec (○) after a step from the resting potential to a potential $V$, are shown in Fig. 5. In agreement with Werblin (1978, 1979) we found a severe outward rectification at potentials positive to −35 mV. This was seen even in the 'instantaneous' (10 msec) $I-V$ relation, although it also

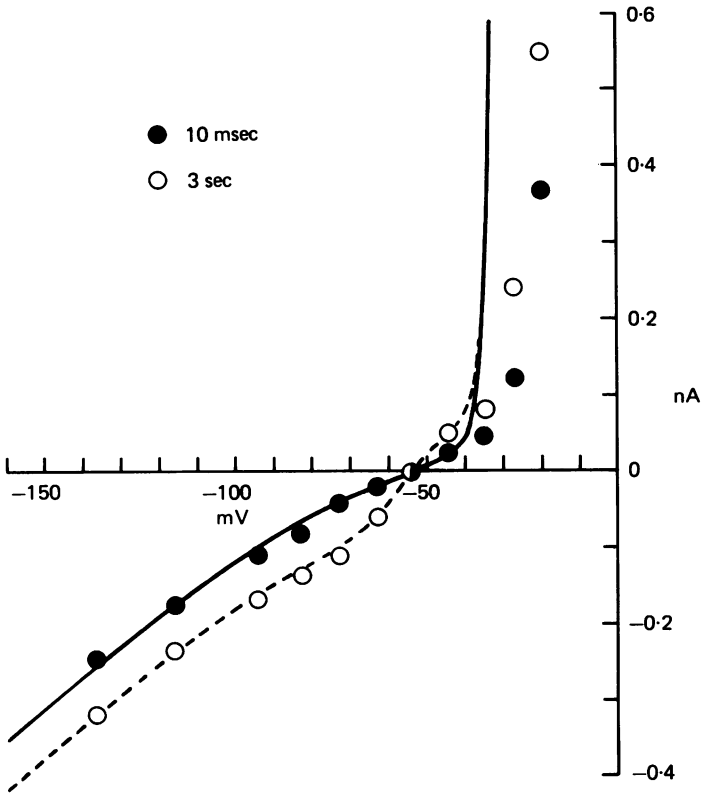


Fig. 5. 'Instantaneous' (●) and steady-state (○) $I-V$ relations for an isolated rod, determined from a holding potential of −54 mV (the resting potential). Negative to −80 mV the $I-V$ relations showed slight inward rectification. Positive to −35 mV there was strong outward rectification. This cell showed outward rectification at an unusually positive potential: on average, in nine cells, the steady-state curve reached 0·5 nA at −35·6 mV. The continuous and broken lines are the instantaneous and steady-state curves predicted by the equations used to simulate the network responses (section *C* in text).

had a slow time-dependent component (see later). The slope resistance was about 10 MΩ in this region. At potentials more negative than −100 mV, inward rectification was generally observed in the $I-V$ relations. It was somewhat variable from cell to cell, and was much weaker than the outward rectification seen at more positive potentials. The general form of the $I-V$ curves (Fig. 5) was similar in over seventy cells, and the voltage-dependence of the time constant and activation curves for the

current $I_A$ (see later) was satisfactorily consistent. Large variations were seen, however, in the input resistance which ranged from 100 to 680 MΩ (measured at the resting potential). Input resistance was loosely correlated with resting potential, which varied from $-45$ to $-70$ mV, and it seems probable that low values of either were usually the result of electrode damage.

As well as the time-independent currents (or rather, currents which reach their steady-state values in less than 10 msec), there was also a conspicuous time-dependent increase of net inward current recorded on hyperpolarizing from the resting potential (Fig. 6*C*). This current is responsible (see Fig. 12) for the 'sag' of the potential observed when a rod is hyperpolarized under current-clamp conditions (Cervetto *et al.* 1977; Werblin, 1978, 1979), and will be called $I_A$. Despite the large range of input resistances encountered, the magnitude of $\bar{I}_A$ (see later), the fully activated time-dependent current, was always close to 0·1 nA in newly penetrated rods. This suggests that, apart from a shunt to ground, low input resistance cells were otherwise normal.

To confirm that the steady-state $I$–$V$ relation for a rod was purely a function of voltage, this curve was sometimes determined twice in the same cell, using two different holding potentials (e.g. $-50$ and $-75$ mV). The two steady-state curves were found to superimpose. This suggests that the history of current flow across the membrane is not a significant factor in determining the $I$–$V$ relation, as it would be, for example, if internal ion concentrations were significantly changed by current flow.

*The time-dependent current, $I_A$, in normal solution*

In Fig. 6 we show the membrane current recorded on clamping the membrane potential to various voltages. For hyperpolarizing pulses from the holding potential ($V_H$, $-68$ mV, the resting potential for this cell), after an 'instantaneous' ($< 10$ msec) current jump there was a time-dependent increase in net inward current. On repolarization to the holding potential a decaying inward (or increasing outward) current tail was seen. The time course of the current was approximately exponential, both at the pulse potential ($V_P$) and at $V_H$ (Fig. 7). In some cells there was a suggestion of an additional small component of slower current change: this was poorly resolved and is ignored hereafter.

As $V_P$ was made more negative, the amplitude of the current tail at $V_H$ initially increased but eventually reached a constant value; making $V_P$ more negative than about $-85$ mV did not increase the tail amplitude further. Depolarizing pulses to potentials below $\sim -40$ mV produced a time-dependent increase in outward current, with an approximately exponential time course. On repolarization to $V_H$ there was a tail of outward current that decayed with the same time constant as the tails after hyperpolarizing pulses. Pulses to more positive potentials produced behaviour that was qualitatively different: the current during the pulse showed a pronounced slow phase, and the kinetics of the tail at $V_H$ were altered. These more positive pulses will be discussed later.

These data suggest that there might be a Hodgkin–Huxley type of gated current

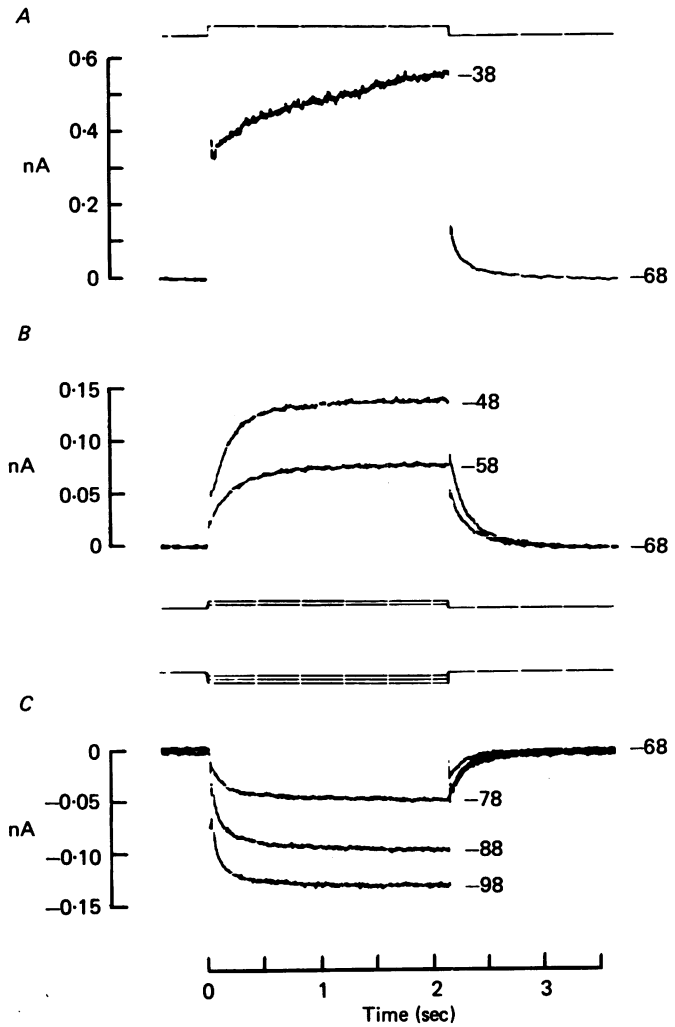


Fig. 6. Membrane current of an isolated rod in response to voltage-clamp steps to various potentials (given at the right of the traces). Resting potential −68 mV in this cell. Voltage is shown as the small rectangular traces. Hyperpolarizing pulses (*C*) activated $I_A$ with a roughly exponential time course. Small depolarizing pulses (*B*) de-activated $I_A$. Large depolarizing pulses (*A*) de-activated $I_A$, but also activated a large, slowly increasing outward current. Note the different current scale in *A*. Temp. 25 °C.

present, with an activation curve spanning the potential range from −85 mV to (at least) −40 mV, and with gating obeying first order kinetics. To investigate this possibility, we postulate that the time-dependent current, which we label $I_A$, can be expressed as

$$I_A[V, t] = \bar{I}_A[V]\, A[V, t], \tag{1}$$

where $I_A[V, t]$ is the current at potential $V$ and time $t$, $\bar{I}_A[V]$ is the fully activated current–voltage relation, i.e. the current which would flow if all the gates controlling

$I_A$ were open, and $A[V, t]$ is a gating variable obeying first-order kinetics, representing the fraction of gates controlling $I_A$ that are open. In the steady-state, the fraction of gates open is defined to be $A_\infty[V]$. Since $A$ obeys first order kinetics, it satisfies the equation

$$dA[V, t]/dt = -(A[V, t] - A_\infty[V])/\tau_A[V], \quad (2)$$

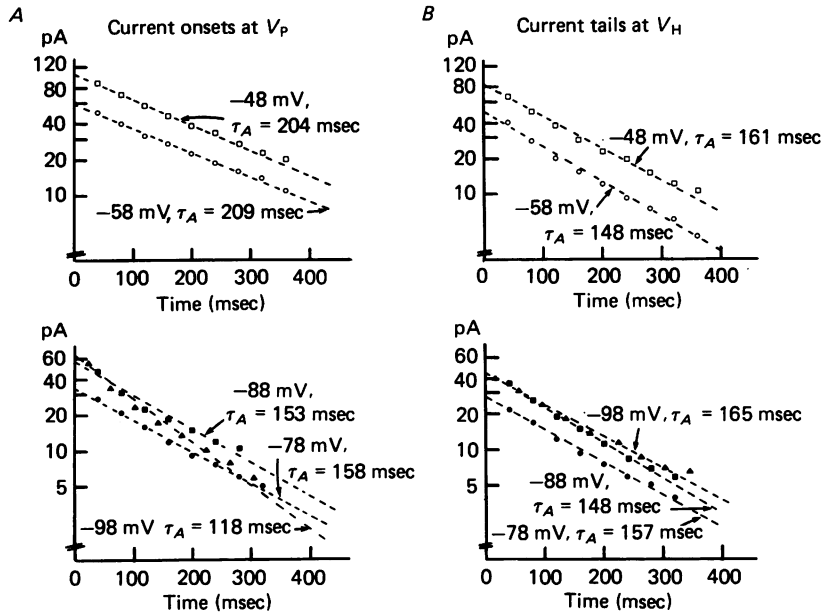


Fig. 7. Semilogarithmic plots of the time course of $I_A$ in Fig. 6. *A*, time course of $I_A$ during pulses away from the holding potential (−68 mV). The current changed roughly exponentially with a time constant that depended on the voltage ($V_P$, given by each curve). *B*, time course of $I_A$ on repolarizing to $V_H$ from different pulse potentials. The time constant was essentially independent of the pulse potential (given by each curve). Plots are not shown for the pulse to −38 mV in Fig. 6, because of contamination from the slow current. All lines fitted by eye.

where $\tau_A[V]$ is the time constant of the change in current at the potential $V$. (See Noble, 1972, for a brief review of Hodgkin–Huxley theory.)

In Fig. 8 we show the results of analysing the current according to this theory. The $\tau_A[V]$ curve (Fig. 8*A*) was derived from semilogarithmic plots of the type in Fig. 7. The time constant should be a unique function of the membrane potential and so should not be affected by the degree to which the current is activated. Thus, the time constant of the current tail recorded at $V_H$ should be independent of the pulse potential $V_P$. To within the scatter of the results, this prediction was satisfied by the data in Fig. 8*B* for potentials more negative than −40 mV. In addition to showing that the gating is purely voltage-dependent, this also implies that there is only one kinetically distinct current present. Data presented later suggests that there are probably at least two, kinetically indistinguishable, currents present but that the description presented here in terms of $I_A$ is formally correct.

The fully activated $\bar{I}_A[V]$ relation was determined using the method of Noble &

Tsien (1968), as follows. Just after a pulse to a potential $V_P$, the change in current is

$$\Delta I[V_P] = \bar{I}_A[V_P]\,(A_\infty[V_P] - A_\infty[V_H]),$$

since the gating variable changes from its steady-state value at $V_H$, to its steady-state value at $V_P$. On returning to $V_H$, the gating variable returns to its original value and the change of current is

$$\Delta I[V_H] = \bar{I}_A[V_H]\,(A_\infty[V_H] - A_\infty[V_P]). \tag{3}$$

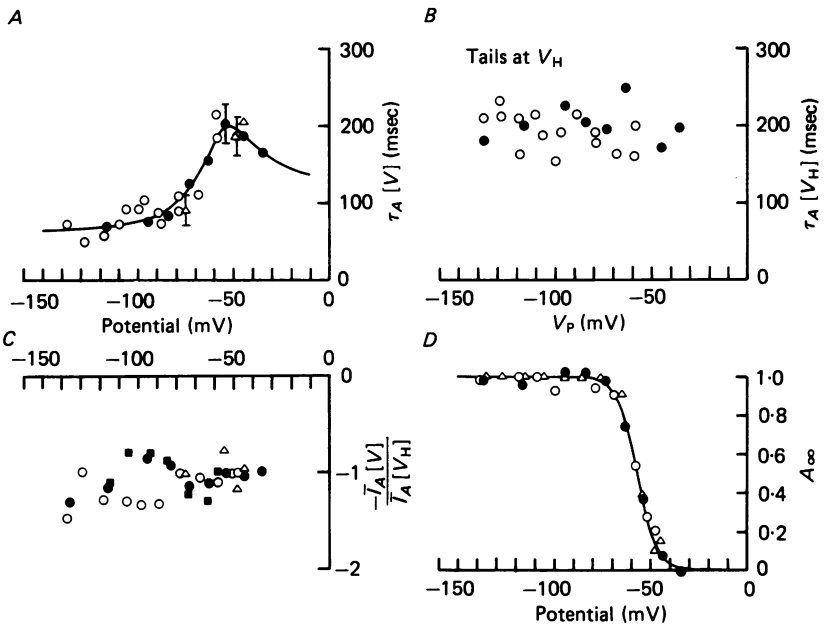


Fig. 8. Characteristics of $I_A$. *A*, time constant, $\tau_A$, as a function of voltage. Data obtained in one cell (●) from a holding potential of −54 mV, and in another cell from $V_H = -48$ (○) and −75 (△). Symbol ● refers to the same cell as Fig. 5. Points with error bars (± 1 S.D.) were obtained from current tails at $V_H$. All other points were obtained during clamp pulses away from $V_H$. *B*, the time constant of the current tail at $V_H$ after a pulse to $V_P$ (abscissa) was approximately independent of $V_P$. Symbols as in *A*. *C*, open channel current $\bar{I}_A$ as a function of voltage, determined from ratio of onset to tail currents for three cells (see eqn. (4)): ●, ○ and △ as above; ■ another cell from $V_H = -58$. *D*, activation curve in two cells from three holding potentials. Symbols as above. Data for the cell with symbols ○ and △ were normalized for consistency with cell ●, since the slow current obscured the bottom of the activation curve. Continuous curves in *A* and *D* are the $\tau_A$ and $A_\infty$ curves (eqns. (7) and (8)) used in simulating the network behaviour.

Taking the ratio of these current changes gives

$$\Delta I[V_P]/\Delta I[V_H] = -\bar{I}_A[V_P]/\bar{I}_A[V_H], \tag{4}$$

which is proportional to the fully activated current–voltage relation at $V_p$. This ratio is plotted in Fig. 8*C*. $\bar{I}_A[V_H]$ is a constant, which can be obtained from the change in current measured when $A$ changes from 0 to 1 (see later). The ratio in

Fig. 8*C* is almost constant, and shows no reversal potential between −40 and −140 mV (as can be seen directly from the raw data of the type shown in Fig. 6). $\bar{I}_A$ could not be determined at potentials more positive than ~ −40 mV because of the presence of the slow current, the kinetics of which are unknown (see later). In some cells $\bar{I}_A$ increased slightly at more negative potentials (see Fig. 8*C*), but in

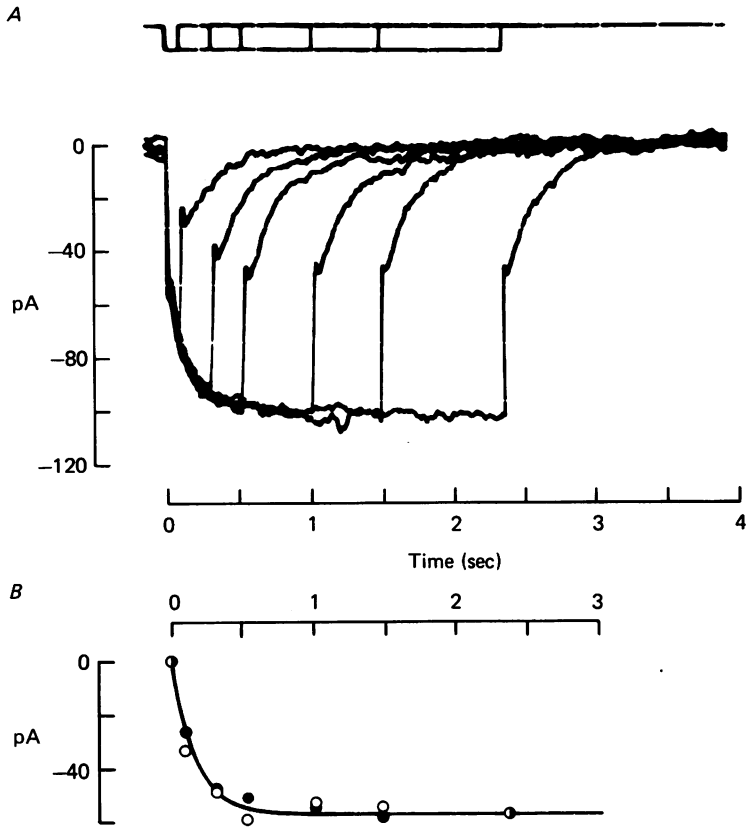


Fig. 9. *A*, upper trace: membrane potential; lower trace: membrane current. Clamp pulses of various durations were applied from $V_H = -54$ mV to $V_P = -74$ mV. *B*, filled circles (●) show the amplitude of the time-dependent current at $V_P$, at the ends of the negative pulses in *A*. Open circles show the amplitudes of the current tails recorded on repolarization to $V_H$ after these negative pulses, multiplied by 0·96. The time course of the increase in tail amplitude paralleled the onset of $I_A$ during the pulse to −74 mV. The continuous curve has the form $-57(1-e^{-t/0{\cdot}164\,sec})$ pA.

others $\bar{I}_A$ decreased slightly at more negative potentials. The slope of the $\bar{I}_A[V]$ relation was always small, and in the simulations described later we take $\bar{I}_A$ to be voltage-independent. Since no ions are known with a reversal potential more negative than −140 mV, it appears that $I_A$ is an inward current in the potential range investigated. Consequently, to explain the time course of the current in Fig. 6, the current must be activated by hyperpolarization. At potentials more negative than ~ −85 mV, therefore, $A_\infty$ is ~ 1.

The entire $A_\infty[V]$ curve was obtained conventionally (e.g. Frankenhaeuser, 1962,

Fig. 1; Noble & Tsien, 1968, fig. 4) from the ratios of the tail currents measured at $V_H$, after 3 sec pulses to various potentials (see eqn. (3)). The normalization coefficient in this analysis is the value of $\bar{I}_A[V_H]$, which was found to be $\sim -0{\cdot}1$ nA (using the convention that outward current is positive). At normal values of the resting potential ($-45$ to $-70$ mV) $A_\infty$ is not zero, and to obtain the bottom of the $A_\infty$ curve it was necessary to measure the current tails following depolarizing pulses. In many rods this procedure was complicated by the fact that, as mentioned above, pulses to potentials more positive than $-40$ or $-35$ mV activated a very slow outward current (discussed later). Changes of this current superimposed on the contribution of $I_A$ to the total membrane current and it was not possible to separate the components satisfactorily. Fortunately, a few rods had only a small slow outward current, so that the tails of $I_A$ could be measured for potentials sufficiently positive that the $A_\infty$ curve was starting to flatten off to zero. The $A_\infty$ curve from such a cell is shown in Fig. 8*D* (●).

To test the consistency of our analysis, which assumes that there is only one kinetically distinct current present, we attempted to study $I_A$ using a holding potential at the top of the activation curve (i.e. $V_H \sim -80$ mV). The gating parameters should depend solely on the membrane potential. We would predict, for example, that the time constant of the decrease of inward current seen on depolarizing from $-80$ to $-60$ mV, should be the same as the time constant of the increase of inward current seen on hyperpolarizing from $-50$ to $-60$ mV. Similarly, the activation curve and $\bar{I}_A[V]$ function should be independent of the holding potential. In three rods a partial kinetic analysis was carried out using a hyperpolarized holding potential, after completion of a full analysis holding at the resting potential. In Fig. 8 (symbols ○ and △) we see that, to within the scatter of the data, the $\tau_A[V]$ curve, the $\bar{I}_A[V]$ curve, and the position on the voltage axis of the top of the $A_\infty$ curve, were independent of the holding potential.

A second check on the consistency of the analysis was provided by the experiment shown in Fig. 9. The magnitude of the current change during a hyperpolarizing pulse was proportional to the amplitude of the tail currents recorded on repolarizing to $V_H$ at various times during the pulse (cf. Hodgkin & Huxley, 1952, fig. 10; Noble & Tsien, 1968, fig. 2). This proportionality is expected if $I_A$ consists of only one kinetically distinct current. It would not hold if there were two currents present with significantly different gating kinetics.

*The time-dependent current, $I_A$, in the presence of caesium and TEA*

Although, in normal solution, $I_A$ apparently behaved as a single gated current, we were surprised that $\bar{I}_A$ was essentially constant over such a large potential range ($-140$ to $-40$ mV), rather than tending towards a reversal potential in the physiological range. Accordingly, we studied $I_A$ further using caesium and TEA, since Werblin (1979) found that these agents affected the voltage response to current injected into isolated rods.

In the presence of 2 mM-CsCl, the time-dependent current seen on hyperpolarizing from the resting potential was an increasing inward current for small potential displacements, as in normal solution. However, as the clamp pulse was made more negative, the amplitude of the current change at the pulse potential decreased and

eventually reversed (Fig. 10*A*). In five rods the average reversal potential was −105·6 mV (S.D. 6·3 mV). An analysis similar to that described above for $I_A$ showed that the time-dependent current remaining in the presence of Cs (which we will label $I_x$) is an outward current, activated by depolarization over the potential range between −80 and −40 mV. The fully activated $\bar{I}_x$ relation was approximately linear

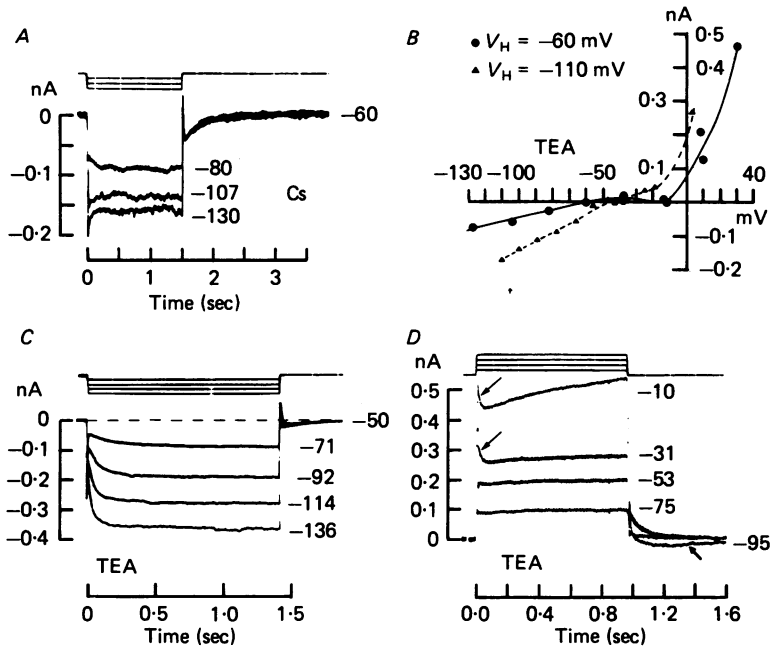


Fig. 10. *A*, currents recorded from an isolated rod in the presence of 2 mM-Cs, on hyperpolarizing from the resting potential (−60 mV). The time-dependent current present reversed between −80 and −107 mV and de-activated by hyperpolarization. Current tails at −60 mV superimposed showing that −80 mV is at the bottom of the $I_x$ activation curve. *B*, instantaneous *I–V* relations obtained in the presence of 15 mM-TEA from two holding potentials in one cell. The curve measured from a $V_H$ where $I_y$ was less activated shows a region of zero slope (●). *C*, currents measured in the presence of 15 mM-TEA on hyperpolarizing to various potentials from $V_H$ = −50 mV. The large onset currents seen at $V_P$ were associated with only small tail currents at $V_H$, indicating a reversal potential positive to −50 mV. *D*, same cell as in *C*, but with $V_H$ = −95 mV. Little time-dependent current was seen during pulses below −40 mV, because of proximity to the reversal potential for $I_y$, but the tails at $V_H$ showed that $I_y$ *was* being de-activated. Larger pulses showed the onset of a reversed $I_y$ (long thin arrows) and also the slow current. The tail at $V_H$ after the pulse to −10 mV showed a slow decreasing inward current (short fat arrow) which is due to the slow current being de-activated below its reversal potential.

with a fully activated conductance of $\bar{g}_x$ = 1·7 nS (S.D. 0·9 nS, $n$ = 5). Cs made the membrane currents more noisy than in normal solution, especially for large hyperpolarizing clamp pulses. This prevented a critical investigation of the kinetics of the current, but at potentials away from the reversal potential (i.e. where the current was large) the current change could be roughly fitted by a single exponential. The voltage dependence of the time constant was similar to that shown for $\tau_A$ in Fig. 8*A*.

The large negative reversal potential for this current suggests that it may be carried by $K^+$ ions, although with our external $K^+$ concentration of 2·1 mM a reversal potential of $-105{\cdot}6$ mV for a $K^+$-specific current would imply an internal $K^+$ concentration of 128 mM, which seems rather high. Within the scatter of the data there was no difference between the resting potentials of rods in the presence of Cs and the resting potentials of rods in normal solution.

Voltage-clamp currents recorded in the presence of 15 mM-TEA solution are shown in Fig. 10*C* and *D*. In addition to removing much of the 'instantaneous' outward rectification at potentials above $-35$ mV, and reducing the resting potential somewhat, TEA also affected the time-dependent current negative to $-40$ mV. Hyperpolarization from a holding potential of $-50$ mV produced a large time-dependent increase of net inward current (Fig. 10*C*), but on repolarizing to $-50$ mV only a small current tail was seen. We label the current, which remains in the presence of TEA, $I_y$. An analysis similar to that described above for $I_A$ showed that in the physiological potential range $I_y$ is an inward current, activated by hyperpolarization between $-40$ and $-80$ mV. The fully activated $\bar{I}_y$ relation was linear, with a fully activated conductance of $\bar{g}_y = 1{\cdot}6$ nS (S.D. 0·4 nS, $n = 4$), and could be extrapolated to a reversal potential at $-32{\cdot}8$ mV (S.D. 6·0 mV, $n = 4$). The kinetics of $I_y$ were found to be approximately exponential. The dependence of the time constant on voltage was very similar to that shown for $\tau_A$ in Fig. 8*A*, and the time constant of the tail at a given holding potential was independent of the potential of the preceding pulse (cf. Fig. 8*B*).

Pulses positive from the resting potential in TEA did not show a significant reversed $I_y$ because the resting potential is near the bottom of the activation curve for the current. However, if large depolarizing pulses were applied from a more negative holding potential (Fig. 10*D*, pulses to $-31$ and $-10$ mV), a rapid decrease of outward current was seen (thin arrows) before the slow outward current turned on. We attribute this to $I_y$ de-activating above its reversal potential. The smaller depolarizing pulses in Fig. 10*D* produced little time-dependent current *during* the pulse away from $-95$ mV. This is because the pulse to $-75$ mV de-activated only a small fraction of $I_y$ (as seen from the small tail at $-95$ mV), while the pulse to $-53$ mV took the membrane potential close to the reversal potential for $I_y$. The pulses to $-53$ and $-31$ mV gave tails at $-95$ mV that almost superimposed, indicating that the bottom of the activation curve for $I_y$ was not far above $-31$ mV. The current tail at $-95$ mV after the pulse to $-10$ mV was biphasic, apparently because $-95$ mV was more negative than the reversal potential for the slow current. Consequently, at late times during the tail (short thick arrow), the current recorded was a slowly decaying inward current, while at earlier times there was a more rapid decay of outward current reflecting both the activation of $I_y$ and the decay of the slow current.

The 'instantaneous' $I$–$V$ relation measured in TEA, from a holding potential near the bottom of the $I_y$ activation curve, often showed a region of zero slope conductance near $-50$ mV (Fig. 10*B*). The 'instantaneous' curve measured from a more negative $V_H$ had a greater slope conductance because $I_y$ was more activated at more negative potentials.

The relationship of the currents $I_x$ and $I_y$ to the current $I_A$ seen in normal solution

is uncertain. An obvious possibility to be considered is that $I_x$ and $I_y$ are independent currents, both present in normal solution, with $I_x$ being blocked by TEA (leaving $I_y$), and $I_y$ being blocked by Cs (leaving $I_x$). $I_A$ would then be the sum of $I_x$ and $I_y$. This idea seemed plausible since, within the scatter of the data, the kinetics of $I_x$, $I_y$ and $I_A$ were not significantly different. Proceeding on this hypothesis, we found that the magnitude and voltage independence of $\bar{I}_A$ could be predicted well by adding together the currents $I_x$ and $I_y$. (For this addition the parameters describing these currents were determined by averaging over five cells in Cs and four cells in TEA.) Unfortunately, however, this approach cannot be completely correct, at least not in its simplest form. If Cs blocks $I_y$ and TEA blocks $I_x$ then both agents together should leave no time-dependent current. Experimentally, however, a small time-dependent current *did* remain in the presence of both drugs. This current was activated by depolarization with a fully activated conductance of $0{\cdot}59 \pm 0{\cdot}36$ nS, and a reversal potential of $-82{\cdot}8 \pm 10{\cdot}5$ mV (mean $\pm$ S.D., $n = 7$ cells). Conceivably a modification of the above hypothesis could account for the presence of this current. For example, TEA and Cs may affect each other's actions, they may only partially block the channels or they may act as charge carriers themselves. Alternatively, there may be more than two gated currents present. We have not pursued these possibilities. Our uncertainty of the number of currents contributing to $I_A$ in no way invalidates the simulation of the rod network data described in section *C* because, in normal solution, $I_A$ behaves as one kinetically distinct current.

*Currents seen with depolarizing pulses*

The strong 'instantaneous' outward rectification occurring positive to $-35$ mV was greatly reduced (but not abolished) by 15 mM-TEA, as reported by Werblin (1979). The well-understood effects of TEA on squid giant axon and frog Ranvier node suggest that this outward rectification is caused by a fast gated $K^+$ current. Time-dependent activation of a fast outward current was not observed during depolarizing pulses. However, if we tentatively assume the TEA-sensitive current in rods (other than $I_x$) to have similar properties to the $K^+$ current in squid giant axon, then at the temperature of our experiments (25 °C) we would expect the time constant of the gating to be less than 0·6 msec (Hodgkin & Huxley, 1952). Our voltage clamp could not resolve changes that are this fast. There may also be a fast *inward* current, which is activated by depolarization too quickly to study with our clamp since, in the presence of TEA, the 'instantaneous' $I$–$V$ relation can show a region of zero slope between $-60$ and $-15$ mV (Fig. 10*B*).

For most rods in normal solution, pulses positive to $-40$ or $-35$ mV produced a slow increase of net outward current during the pulse, and a slow tail on returning to the holding potential (Figs. 6 and 11). At late times during these tails, when $I_A$ was presumed to be constant, the slow current decayed approximately exponentially (Fig. 11), with a time constant between 1 and 5 sec. The size of the slow current tail at holding potentials around $-50$ mV was much smaller than the slow change in current during the depolarizing pulse, suggesting that the reversal potential for the slow current is negative to $-50$ mV, and hence that this is an outward current activated by depolarization. Use of a more negative holding potential in normal solution did not give a convincing reversal of the slow current tail. In the presence of TEA, pulses to

more positive potentials can be made. These activated more slow current, and gave a larger slow current tail at $V_H$, which could be more readily distinguished from drift of the current baseline. With TEA present, reversal of the slow current tail was sometimes observed at holding potentials more negative than $-70$ mV (e.g. Fig. 10*D*, tail from $V_P = -10$ mV). The slow current was still observed in the presence of 2 mM-Cs.

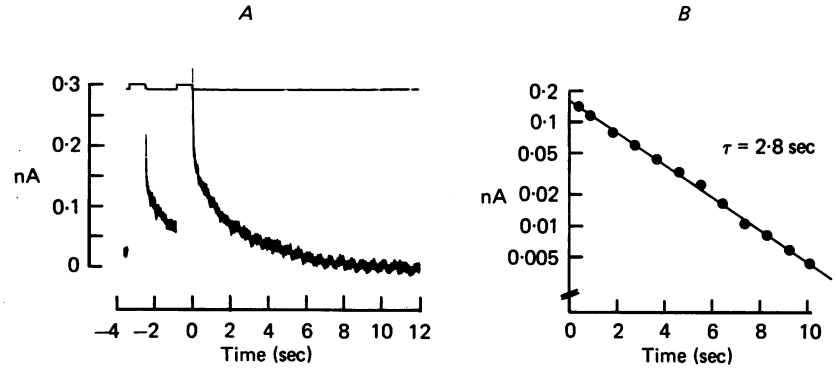


Fig. 11. Time course of slow current tail at $V_H = -50$ mV. *A*, a train of voltage-clamp pulses to $-30$ mV (upper trace) was applied to produce substantial activation of the slow current. Currents at $-30$ mV were off screen. *B*, the slow phase of the tail was fitted (by eye) with a single exponential with a time constant of 2·8 sec. At early times during the tail at $V_H$ there was a rapid component to the current decay.

### *C. Simulation of the network behaviour using the voltage-clamp data*

The data presented in the previous section give a reasonably complete description of the membrane currents in isolated rods. In this section we will use these results to investigate whether the rod membrane properties are sufficient to explain the response of the rod network to current injection, and to investigate the role of $I_A$ in shaping the light response.

#### *The response of isolated rods to current injection*

As a first step in simulating the network behaviour, we will test the validity of our voltage-clamp analysis by simulating the voltage responses recorded in isolated rods under current-clamp conditions. Fig. 12*A* shows the response of a rod to current pulses in multiples of $\pm 0{\cdot}085$ nA. The predicted responses, based on voltage-clamp data obtained from the same cell, are shown in Fig. 12*B*.

The curves were obtained by solving the equation determining the membrane potential, $V$, at time, $t$, i.e.

$$C\mathrm{d}V/\mathrm{d}t = I_{\mathrm{inj}}[t] - I_{\mathrm{i}}[V, t], \tag{5}$$

where $C$ is the cell capacitance (40 pF), $I_{\mathrm{inj}}$ is the injected current, and $I_{\mathrm{i}}$ is the outward ionic current across the cell membrane. Since, in normal solution, the time dependence of the membrane current can be described in terms of a single gated current $I_A$, we represented $I_{\mathrm{i}}$ as the sum of two terms:

$$I_{\mathrm{i}}[V, t] = I_{\mathrm{leak}}[V] + \bar{I}_A[V]\, A[V, t], \tag{6}$$

where $I_{leak}[V]$ is the time-independent membrane current (i.e. including any current activated too quickly to be resolved by our clamp), and $A$ satisfies eqn. 2. The slow current will be ignored in this and later simulations, because (i) we were unable to characterize it adequately and (ii) its omission has only a small effect on the predicted voltage responses because of the strong outward rectification in the $I_{leak}[V]$ relation. In this rod, the $A_\infty[V]$ and $\tau_A[V]$ curves were approximately described by the empirical expressions

$$A_\infty[V] = 1/\{1+\exp((V+57)/5)\}, \tag{7}$$

$$\tau_A[V] = 0{\cdot}06+0{\cdot}14/\{1+(V+53)^2/289\} \quad \text{for} \quad V < -53, \tag{8a}$$

$$\tau_A[V] = 0{\cdot}12+0{\cdot}08/\{1+(V+53)^2/500\} \quad \text{for} \quad V > -53, \tag{8b}$$

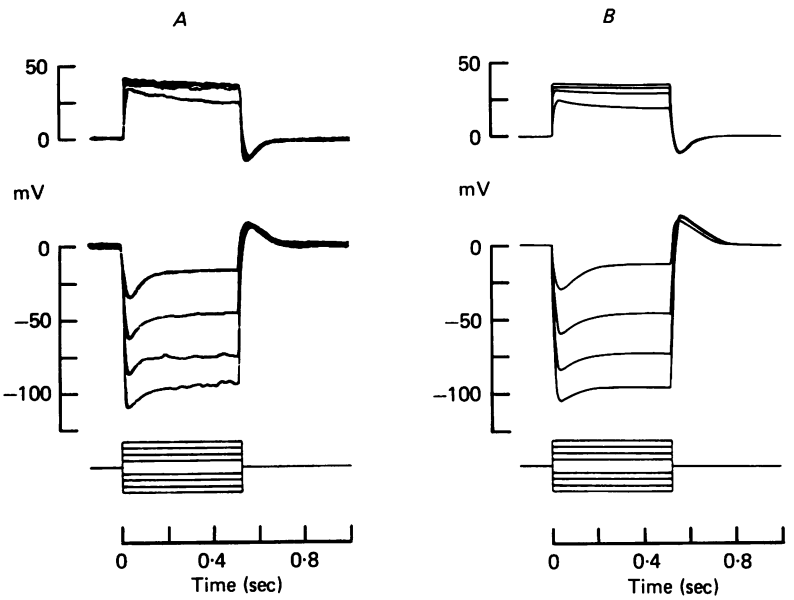


Fig. 12. *A*, measured voltage responses (upper trace) of an isolated rod to current pulses of ±0·085, ±0·17, ±0·255 and ±0·34 nA (lower trace). Resting potential −54 mV. *B*, predicted responses based on voltage-clamp data derived from the same cell. See text pp. 306–308 for details of the simulation.

with $V$ in mV, and $\tau_A$ in sec. These curves are shown in Fig. 8. $\bar{I}_A$ was set to −0·108 nA. This is 12% higher than was obtained in the voltage-clamp experiments on the same cell, which were done *after* the current-clamp experiments: this small increase is an attempt to compensate for the slow decline of $\bar{I}_A$, observed during most experiments, as the cell's condition deteriorates. The $I_{leak}[V]$ curve can be obtained, either (i) by subtracting $\bar{I}_A[V]A_\infty[V_H]$ from the 'instantaneous' $I$–$V$ relation measured on clamping to various potentials, $V$, from $V_H$, or (ii) by subtracting $\bar{I}_A[V]A_\infty[V]$ from the steady-state $I$–$V$ relation. Negative to $\sim -40$ mV, where there is no contamination from the slow current, these procedures give the same result. At more positive potentials the former procedure was used, to minimize contamination from the slow current. For $V \geqslant -95$ mV, $I_{leak}[V]$ was approximated by the empirical expression

$$I_{leak}[V] = (V+71{\cdot}743)/464+0{\cdot}00988\exp((V+35)/5), \tag{9a}$$

with $V$ in mV and $I_{leak}$ in nA. The first term accounts for the linear part of the $I$–$V$ relation near the resting potential (resistance 464 MΩ in this cell), and the second term accounts for the outward rectification positive to −40 mV (which was rather weak in this cell). The resting potential was −54 mV. For $V \leqslant -95$ mV, a term

$$-0{\cdot}0001614\,(-V-95)^{1{\cdot}5} \tag{9b}$$

was added to the expression above, to take account of the inward rectification in this potential range. This description of the inward rectification was derived from the steady-state $I$–$V$ relation obtained from the current-clamp data in Fig. 12$A$; it is slightly different from the description used later in simulating the network responses, which was based on the voltage-clamp data obtained later from the same cell (Fig. 5).

Although there are some differences between the experimental and predicted responses in Fig. 12, the agreement is generally quite good. In particular, the sag of the potential during hyperpolarizing pulses is reproduced satisfactorily, the time-to-peak of the responses (40–50 msec for hyperpolarizing pulses) is correctly predicted and the overshoot potential at the end of the current pulse is predicted to be almost independent of the magnitude of the current, as observed. (This last prediction is only expected for current pulses large enough to polarize the membrane near to, or past, the ends of the $A_\infty$ curve). The relatively minor discrepancies between the time courses and magnitudes of the theoretical and experimental responses are attributable to slight changes in the properties of the rod between performing the current-clamp and voltage-clamp experiments. For depolarizing pulses the omission of the slow current, and uncertainty in the exact position of the bottom of the $A_\infty$ curve (because of the presence of the slow current, see p. 302), must also contribute to the small differences observed. This satisfactory fit of the current-clamp data suggests that the voltage-clamp data provide a reasonably accurate description of the membrane properties of isolated rods.

*The network response to current injection*

To simulate the network response to current injection we treated the rods as being in a square array,with electrical coupling between next neighbour rods (see Fig. 1). The presence of cones was ignored in this simulation (see Discussion). In the absence of any direct information on the rod coupling mechanism, we assumed the current flow between neighbouring cells to be proportional to the difference in potential of the rods (ohmic resistive coupling).

Each rod's membrane potential satisfies an equation of the form

$$C\mathrm{d}V_{i,j}/\mathrm{d}t = -I_i[V_{i,j}, t] - g_c(V_{i,j}-V_{i-1,j}) - g_c(V_{i,j}-V_{i+1,j}) - g_c(V_{i,j}-V_{i,j-1}) - g_c(V_{i,j}-V_{i,j+1}). \quad (10)$$

The last four terms are the current leaving the $\mathrm{rod}_{i,j}$ to pass to its next neighbours through junctions of conductance $g_c$. For the rod where current is injected ($\mathrm{rod}_{0,0}$) a term $I_{inj}[t]$ must be added to the right hand side of (10). The extracellular space is assumed to be isopotential. We based our description of $I_i[V, t]$ in (10) on data from isolated rods which had an input resistance greater than 450 MΩ, believing these to have been least damaged by the electrodes. $\bar{I}_A$ was set at $-0{\cdot}096$ nA. The $A_\infty$ and $\tau_A$ functions used were as described above for simulation of the isolated rod responses, and are shown in Fig. 8. The $I_{leak}$ curve was modified slightly from eqn. (9) to give more outward rectification at depolarized potentials and more inward rectification at large negative potentials, as generally observed (see legend to Fig. 5). The relation used was

$$I_{leak}[V] = (V+69{\cdot}7839)/464 + 0{\cdot}0164 \exp((V+40)/2) \quad \text{for} \quad V \geqslant -75\ \text{mV},$$
$$\text{with a term} \quad -0{\cdot}0001614\,(-V-75)^{1{\cdot}5} \quad \text{added for} \quad V < -75\ \text{mV}; \quad (11)$$

$V$ is in mV and $I_{leak}$ in nA. The 'instantaneous' and steady-state $I$–$V$ relations predicted from these $A_\infty$, $\bar{I}_A$ and $I_{leak}$ functions are shown in Fig. 5. The simultaneous eqns. (2), (6), (7), (8), (10) and (11) were solved for all the rods in a thirteen rod by thirteen rod array, centred on $\mathrm{rod}_{0,0}$. Rods outside this area were assumed to remain at the resting potential ($-54$ mV). The

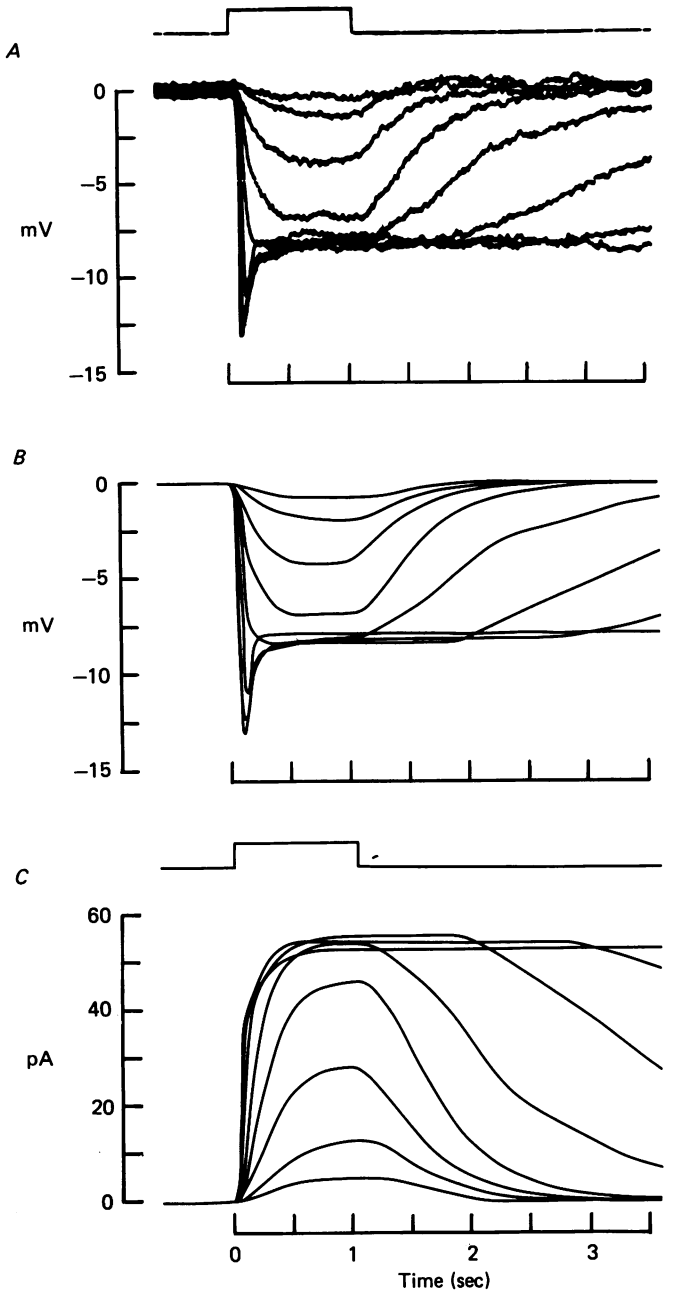


Fig. 13. *A*, voltage response of a rod in the network to broad field illumination delivered through the microscope objective. Stimuli were 1·04 sec flashes of white light. Log intensity increased successively in increments of 0·5. Resting potential −59 mV. *B*, analytical curves fitted to data in *A* after correction for base-line drift. Particular care was taken to fit the upstroke and peak of the responses to within 5%. *C*, photocurrents which we calculate to have produced the responses in *A*, by using the analytical fits of *B* in eqn. (12).

symmetry of the array allows the equations to be solved by considering only twenty-eight rods in one octant of the thirteen by thirteen array. The only parameter in the equations which could not be measured directly is the coupling resistance $1/g_c$. The value of $1/g_c$ was set to 300 MΩ, to approximately reproduce the peaks of the voltage responses in $rod_{0,0}$.

The results of the simulation, for injection of current pulses of ± 1 nA and ± 2 nA into $rod_{0,0}$, are shown in Fig. 2*B*. The agreement with Fig. 2*A* is by no means perfect, but the main features of the responses are reproduced well. The most important discrepancies between experiment and simulation are (i) that the responses for more distant rods showed a higher ratio of peak response to sustained response than is predicted, and (ii) that the simulations predict the time to the peak of the response, to a 1 nA hyperpolarizing pulse, to increase from 31 msec at $rod_{0,0}$ to 48 msec at $rod_{4,0}$ while, on average, the experimental values were 44 msec and 70 msec respectively. It should be borne in mind that in carrying out the simulations the following simplifications have been made: (1) the voltage-clamp data were obtained from rods without axons, (2) we have ignored rod–cone coupling (see Discussion) and the slow current, (3) we have assumed ohmic coupling between rods, although the coupling could be voltage- and time-dependent (cf. Spray, Harris & Bennett, 1979), (4) we have assumed a regular geometry for the rod connexions, with no breaks in the lattice see Fig. 1).

*The light-induced current during broad field stimulation*

During broad field illumination there is no lateral current flow through rod–rod connexions, so the rods can be treated as isolated (neglecting rod–cone coupling). From the voltage response, $V[t]$, of the rod network to such stimulation, the membrane current elicited in each rod by light can be obtained as

$$I_{light}[t] = -C\,dV/dt - I_i[V,t] \tag{12}$$

where $I_i$ is the ionic current which would flow at $V[t]$ in the absence of illumination, and is given by eqns. (2), (6), (7), (8) and (11). If the only effect of light is to close $n[t]$ sodium channels at time $t$, each of which has an $I$–$V$ relation $\bar{I}_{Na}[V]$ when open, then the current derived by this method is

$$I_{light}[t] = -n[t]\bar{I}_{Na}[V\,[t]]. \tag{13}$$

Unless $\bar{I}_{Na}$ is voltage-independent, this is *not* the current which would be recorded under voltage-clamp conditions, because the membrane potential is varying with time. If there are no ionic channels in the outer segment other than those which can be blocked by light, the current obtained in this way should equal that measured as flowing through the outer segment, by the method of Baylor, Lamb & Yau (1979), during broad field illumination.

In Fig. 13*A* we show the network response to broad field illumination, measured in the isolated retina preparation with 1·04 sec flashes of white light of various intensities. Fig. 13*C* shows the calculated photocurrents needed to produce these responses. While the voltage responses to the brighter flashes show a distinct peak-plateau sequence, the photocurrent does not, consistent with the results of Baylor *et al.* (1979, Fig. 5*B*), in the toad. The decline of the potential from the peak of the voltage response to bright flashes is produced by $I_A$. The rising phase of the photocurrent is faster for brighter flashes.

*Spread of the light response through the network*

Detwiler *et al.* (1978) found that when a bar of light was flashed on the rod network of the turtle, the peak of the voltage response occurred earliest in rods that were furthest from the stimulus. To investigate whether this could be produced by a current like $I_A$, we simulated the effect of illuminating the salamander rod network with a bar of light incident upon the row of rods extending through $rod_{0,0}$ and $rod_{0,6}$ in Fig. 1. The voltage response in $rod_{0,0}$ was taken as

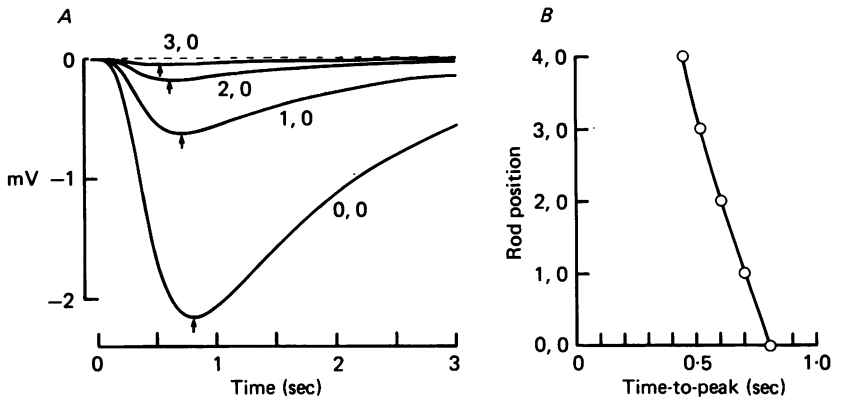


Fig. 14. *A*, simulated photoresponses in the row of rods through $rod_{0,0}$ and $rod_{6,0}$, when a light bar falls on the row perpendicular to this through $rod_{0,0}$. Voltage response in $rod_{0,0}$ was taken from figure-legend 6 of Detwiler *et al.* (1978). *B*, times-to-peak are shorter in the more distant rods, giving a negative conduction velocity as observed experimentally by Detwiler *et al.* (1978). This is produced by $I_A$.

$$\Delta V_{0,0}[t] = -4{\cdot}35\,(\exp(-0{\cdot}135t) - \exp(-4{\cdot}49t))^5,$$

as found by Detwiler *et al.* (1978, Fig. 6), and the resulting responses in the row of rods through $rod_{0,0}$ and $rod_{6,0}$ in Fig. 1 were calculated. The membrane properties and coupling conductance assumed were the same as for simulating the network responses to current injection. Rods further away than $rod_{8,0}$ were assumed to remain at the resting potential (−54 mV). No current flows through rod–rod connexions parallel to the light bar.

As shown in Fig. 14, the predicted responses peak earlier in rods that are further away from $rod_{0,0}$, as observed by Detwiler *et al.* (1978). This phenomenon is a consequence of the light response having a rise time which is comparable with the time constant of $I_A$: for injection of a current *step* into $rod_{0,0}$ the responses peak *later* in rods that are further away, as is expected for a network of resistors and capacitors. The responses we calculate decrement more quickly with distance than those found by Detwiler *et al.* (1978) presumably because in the turtle the rod coupling resistance is lower, or the rod membrane resistance is higher, than in the salamander.

## DISCUSSION

### *The rod membrane currents*

The rod membrane properties we observed under voltage-clamp conditions are generally consistent with those found by Werblin (1979) using the current-clamp method. We found higher membrane resistances than he did, presumably because the cells were less damaged by the electrodes. In agreement with Werblin, we observed strong outward rectification for potentials more positive than about $-35$ mV, while Bader *et al.* (1978) only observed a smaller rectification positive to 0 mV. It is possible that the enzyme treatment used by Bader *et al.* (1978) to isolate whole rods degraded the fast $K^+$ channels postulated to be responsible for the outward rectification, since the outward rectification we saw in the presence of TEA is similar to that found by them. Alternatively, the axon terminals may contribute a strong inward current at potentials more positive than $\sim -35$ mV, which would not be seen in our rods with detached axons. The observation of strong outward rectification in intact rods that are coupled to the rod network (Fig. 2*A*; Werblin, 1975) argues against the latter possibility however.

For rods in normal solution, Werblin (1979) could not detect a time-dependent change in membrane resistance during the voltage response to a hyperpolarizing current. This is consistent with our observation that $\bar{I}_A$ is approximately independent of voltage, which we tentatively attribute to $I_A$ being the sum of at least two currents, one of which is activated by hyperpolarization and one of which is activated by depolarization.

In the presence of Cs, Werblin (1979) found a time-dependent increase of resistance on hyperpolarization, as we expect since the current $I_x$ left in Cs is an outward current de-activated by hyperpolarization. Fain *et al.* (1978) found that, in the toad retina, Cs increased the rod response to light, and removed the peak–plateau sequence for bright flashes. This is also what we would predict: the remaining time-dependent current ($I_x$) will still tend to reduce the light response, but the brightest flashes take the membrane potential close to the reversal potential for $I_x$, so that the large changes in gating of this current have only a small effect on the voltage wave form, while dimmer flashes do not de-activate $I_x$ sufficiently quickly to produce a noticeable peak–plateau sequence.

Werblin (1979) found that TEA removed the peak–plateau sequence of the voltage response to a hyperpolarizing current, in the potential range between $-30$ and $-70$ mV. We do not find a complete removal of the peak–plateau sequence in this range, but there is a reduction in the sag of the voltage response, presumably because the potential is close to the reversal potential for the remaining current $I_y$. Fain *et al.* (1977) have reported that TEA induces regenerative activity in rods of the intact toad retina. This never occurred in our isolated rods, but we have observed a region of zero slope in the 'instantaneous' $I$–$V$ relation measured in TEA (Fig. 10*B*), which could be due to the presence of a fast inward current. Such a current might be responsible for initiating the action potentials that Fain *et al.* (1977) found.

*Rod–cone coupling*

We have ignored the presence of rod–cone coupling in our simulation of the network behaviour, because insufficient information is available on the properties of individual cones. When current is injected into a rod in the retinal slice preparation, the voltage response in a neighbouring cone is about a third of that in a neighbouring rod (Fig. 3). This does not necessarily imply, however, that the presence of the cones significantly affects the response of the rod network to current injection: the voltage response in the neighbouring cone depends not only on the rod–cone coupling conductance, but also on the coupling connectivity of the cones and the cone membrane resistance, neither of which are known. The results of Fain (1976) suggest that, in *Bufo* at least, current flow between the rod and cone systems is small.

*The functional role of* $I_A$

The time-dependent current $I_A$ affects signal shaping in the rod network in two conceptually different ways.

The purely temporal effects of $I_A$ are apparent when the rod network is uniformly illuminated. $I_A$ is responsible for the peak–plateau sequence of the voltage response to bright flashes (Fig. 13). Adaptive behaviour of this type, in response to strong stimuli, is a property of many receptor systems. One of its functions in the rods may be to keep the membrane potential within the operating range of the synapse to second-order cells. The kinetics of $I_A$ become faster at more negative potentials. This suggests that the time course of the peak–plateau sequence is matched to the time course of the photocurrent, which becomes faster for bright flashes (Fig. 12; Baylor *et al.* 1979) and when light-adapted (Baylor & Hodgkin, 1974). It is curious that $I_A$ is apparently not a single current, but is instead the sum of at least two opposing conductances, resulting in the fully activated $\bar{I}_A[V]$ being almost voltage-independent. The evolution of such a mechanism may have been advantageous for two reasons. First, it allows a peak–plateau sequence to occur over a wide range of potentials, without being limited by the reversal potential of the current responsible. Secondly, it results in the sag of the light response being accompanied by little or no conductance change, so that the rod sensitivity to a subsequent flash will not be altered greatly. If, for example, the sag were produced solely by the activation of an inward sodium current, the concomitant increase in membrane conductance would reduce the voltage response to a later flash.

In the case of localized illumination of the retina, the current $I_A$ shapes the photoresponse as it propagates laterally through the rod network (Fig. 14). In general, $I_A$ makes the response more transient as it spreads laterally. In addition, as observed by Detwiler *et al.* (1978) in the turtle retina, and as our model predicts, the peak of the response can occur earlier in rods that are further away from an illuminated area of the retina.

Previously, it has often been suggested that the functional role of rod coupling is to improve the reliability of signals transmitted to second-order cells, especially when few photons are absorbed. The processing in time and space that the rod network performs on incoming signals, at all intensities up to rod saturation, may be equally important for visual function.

David Attwell is a post-doctoral research fellow of the Science Research Council, U.K. This work was supported by an N.E.I. academic investigator award (K07 EY 00159) to Martin Wilson and N.E.I. grant EY 00561 to Frank Werblin. We are grateful to the University of California, Berkeley for subsidizing the computer time used in this project.

## REFERENCES

BADER, C. R., MACLEISH, P. R. & SCHWARTZ, E. A. (1978). Responses to light of solitary rod photoreceptors isolated from tiger salamander retina. *Proc. natn. Acad. Sci. U.S.A.* **75**, 3507–3511.

BAYLOR, D. A., FUORTES, M. G. F. & O'BRYAN, P. M. (1971). Receptive fields of single cones in the retina of the turtle. *J. Physiol.* **214**, 265–294.

BAYLOR, D. A. & HODGKIN, A. L. (1974). Changes in time scale and sensitivity in turtle photoreceptors. *J. Physiol.* **242**, 729–758.

BAYLOR, D. A., LAMB, T. D. & YAU, K.-W. (1979). The membrane current of single rod outer segments. *J. Physiol.* **288**, 589–611.

BROWN, J. E. & PINTO, L. H. (1974). Ionic mechanism for the photoreceptor potential of the retina of *Bufo marinus*. *J. Physiol.* **236**, 575–591.

BROWN, P. K., GIBBONS, R. I. & WALD, G. (1963). The visual cells and visual pigments of the mudpuppy, *Necturus*. *J. cell Biol.* **19**, 79–106.

CERVETTO, L. & MACNICHOL, E. F., JR. (1972). Inactivation of horizontal cells in turtle retina by glutamate and aspartate. *Science, N.Y.* **178**, 767–768.

CERVETTO, L., PASINO, E. & TORRE, V. (1977). Electrical responses of rods in the retina of *Bufo marinus*. *J. Physiol.* **267**, 17–51.

COPENHAGEN, D. R. & OWEN, W. G. (1976). Functional characteristics of lateral interactions between rods in the retina of the snapping turtle. *J. Physiol.* **259**, 251–282.

CUSTER, N. V. (1973). Structurally specialised contacts between the photoreceptors of the retina of the axolotl. *J. comp. Neurol.* **151**, 35–56.

DENNIS, M. J. & SARGENT, P. B. (1979). Loss of extrasynaptic acetylcholine sensitivity upon reinnervation of parasympathetic ganglion cells. *J. Physiol.* **289**, 263–275.

DETWILER, P. B., HODGKIN, A. L. & MCNAUGHTON, P. A. (1978). A surprising property of electrical spread in the network of rods in the turtle's retina. *Nature, Lond.* **274**, 562–565.

FAIN, G. L. (1975). Quantum sensitivity of rods in the toad retina. *Science, N.Y.* **187**, 838–841.

FAIN, G. L. (1976). Sensitivity of toad rods: dependence on wave-length and background illumination. *J. Physiol.* **261**, 71–101.

FAIN, G. L., QUANDT, F. N., BASTIAN, B. L. & GERSCHENFELD, H. M. (1978). Contribution of a caesium-sensitive conductance increase to the rod photoresponse. *Nature, Lond.* **272**, 467–469.

FAIN, G. L., QUANDT, F. N. & GERSCHENFELD, H. M. (1977). Calcium-dependent regenerative responses in rods. *Nature, Lond.* **269**, 707–710.

FRANKENHAEUSER, B. (1962). Potassium permeability in myelinated nerve fibres of *Xenopus laevis*. *J. Physiol.* **160**, 54–61.

GOLD, G. H. (1979). Photoreceptor coupling in retina of the toad *Bufo marinus*. II. Physiology. *J. Neurophysiol.* **42**, 311–328.

GOLD, G. H. & DOWLING, J. E. (1979). Photoreceptor coupling in retina of the toad *Bufo marinus*. I. Anatomy. *J. Neurophysiol.* **42**, 292–310.

HINDMARSH, A. C. & BYRNE, G. D. (1977). EPISODE: an effective package for the integration of systems of ordinary differential equations. *Lawrence Livermore Laboratory, report* UCID-30112, P.O. Box 808, Livermore, CA 94550, U.S.A.

HODGKIN, A. L. & HUXLEY, A. F. (1952). The components of membrane conductance in the giant axon of *Loligo*. *J. Physiol.* **116**, 473–496.

LAMB, T. D. & SIMON, E. J. (1976). The relation between intercellular coupling and electrical noise in turtle photoreceptors. *J. Physiol.* **263**, 257–286.

LASANSKY, A. & MARCHIAFAVA, P. L. (1974). Light-induced resistance change in retinal rods and cones of the tiger salamander. *J. Physiol.* **236**, 171–191.

MARSHALL, L. M. & WERBLIN, F. S. (1978). Synaptic transmission to the horizontal cells in the retina of the larval tiger salamander. *J. Physiol.* **279**, 321–346.

NOBLE, D. (1972). Conductance mechanisms in excitable cells. *Biomembranes*, vol. 3, ed. KREUZER F. & SLEGERS, J. F. G., pp. 427–447. New York: Plenum.

NOBLE, D. & TSIEN, R. W. (1968). The kinetics and rectifier properties of the slow potassium current in cardiac Purkinje fibres. *J. Physiol.* **195**, 185–214.

NORMANN, R. A. & POCHOBRADSKÝ, J. (1976). Oscillations in rod and horizontal cell membrane potential: evidence for feed-back to rods in the vertebrate retina. *J. Physiol.* **261**, 15–29.

OWEN, W. G. & COPENHAGEN, D. R. (1977). Characteristics of the electrical coupling between rods in the turtle retina. In *Vertebrate Photoreceptors*, ed. BARLOW, H. B. & FATT, P. London: Academic Press.

SCHWARTZ, E. A. (1975*a*). Rod–rod interaction in the retina of the turtle. *J. Physiol.* **246**, 617–638.

SCHWARTZ, E. A. (1975*b*). Cones excite rods in the retina of the turtle. *J. Physiol.* **246**, 639–651.

SCHWARTZ, E. A. (1976). Electrical properties of the rod syncytium in the retina of the turtle. *J. Physiol.* **257**, 379–406.

SJÖSTRAND, F. S. & KREMAN, M. (1978). Molecular structure of outer segment disks in photoreceptor cells. *J. ultrastruct. Res.* **65**, 195–226.

SPRAY, D. C., HARRIS, A. L. & BENNETT, M. V. L. (1979). Voltage dependence of junctional conductance in early amphibian embryos. *Science, N.Y.* **204**, 432–434.

WALLS, G. L. (1942). *The Vertebrate Eye and Its Adaptive Radiation*. New York: Hafner. (Reprinted 1967).

WERBLIN, F. S. (1975). Regenerative hyperpolarization in rods. *J. Physiol.* **244**, 53–81.

WERBLIN, F. S. (1978). Transmission along and between rods in the tiger salamander retina. *J. Physiol.* **280**, 449–470.

WERBLIN, F. S. (1979). Time- and voltage-dependent ionic components of the rod response. *J. Physiol.* **294**, 613–626.